ADVANCES IN SIMULATING RADIATIVE TRANSFER IN COMPLEX ENVIRONMENTS

Accurate modelling of radiative fluxes plays an important role in microclimatology. This is especially the case in urban areas, where large differences in radiative fluxes can be found due to the complex structures and the multitude of different surface types. While primary radiative transfer, i.e. incoming shortwave and longwave radiation, can be simulated quite easily using ray tracing algorithms and local Sky View Factors, simulating secondary radiative fluxes which are emitted or reflected by objects of the environment (walls, roofs, the ground surface or vegetation) are much more complicated to model.

The complexity in modelling these radiative fluxes lies in the multiple interactions between the different elements within the view range of the grid analysed. For instance, radiation reflected by a surface will contribute to the incoming radiation received by other surfaces. These surfaces will again also re-reflect parts of this radiation and distribute in vicinity. Handling such complex conditions is a challenge that is common to all algorithms that involve simulating multiple reflections of radiation such as daylight simulation or image rendering in general.

In previous versions, the distribution of secondary radiative fluxes (reflected shortwave radiation and longwave radiation emitted from objects) was calculated using Averaged Viewfactors (AVF). In the AVF concept, first view factors were calculated for all grid cells using a 3d ray tracing for 10° height and azimuth angle facets.
(→ see Figure 1).

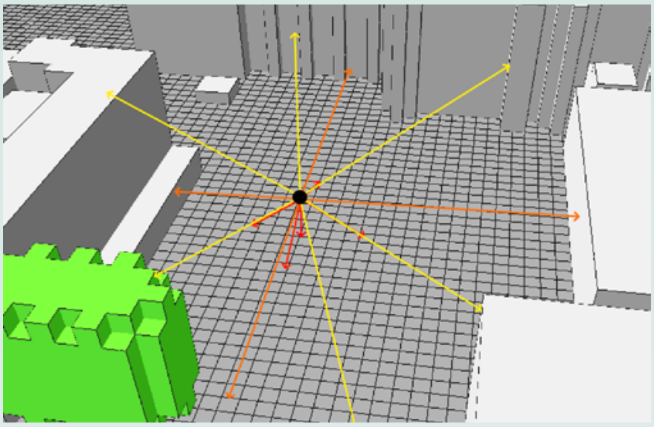

→ **Figure 1**: Three-dimensional ray tracing is performed for every grid cell in the model area. Based on the objects hit, the view factors for that cell are calculated.

Based on the object type (sky, building, plant, ground surface) hit by a ray and the total number of rays traced, averaged view factors of sky, vegetation, buildings and ground surfaces were stored as single values for each grid cell. A direct link between individual objects hit by the ray in a particular facet (i.e. facades, plant sections or ground surfaces) however was, to save memory and computational time, not stored.

This however comes at a huge downside: By only storing the fraction of buildings, plants, ground surfaces "seen" by a grid cell, the information which particular building surface, plant section or ground surface can be seen by the grid cell is lost.
Thus, instead of individual information of radiation received from particular objects, the emitted secondary radiation was averaged over the complete model domain and then combined with a grid cells' view factor for buildings, plants and ground surfaces. As a consequence, every point with an identical view factor for buildings, ground surfaces or vegetation will receive the same amount of reflected radiation at a given time.

This oversimplification led to very unrealistic results, where e.g. given the same view factors, locations in front of high-reflective walls would receive the same reflected radiation compared to darker walls.

To overcome this simplification, a new algorithm called the Indexed View Sphere (IVS) was developed and implemented into ENVI-met. The main idea behind IVS is to efficiently save the results of the individual facets making up the view factor and thus enable backlinking the contributing elements of the urban environment. By storing not only the type of element seen by the cell, but also a reference pointer to the exact building surface, plant cluster and ground surface is saved. Using this pointer, the actual state of the objects seen by the grid cell can be used to calculate the received secondary radiative fluxes. Furthermore, a visibility factor that alters the radiation received has been added. This visibility factor accounts for partial obstruction caused by leaves.

Similar to the former AVS routine, the pointer calculation of the IVS only needs to be performed once during a model run. When the visibility analysis of the facets is completed and the reference pointers are stored, only actual reflected shortwave radiation and longwave radiation emitted by the objects needs to be updated in order to receive secondary radiative fluxes of the analysed point.

Storing reference pointer and visibility information for every facet of a 3d ray tracing leads to immense memory demand. Even for smaller model areas of 200 x 200 x 35 grids around one billion data records need to be stored when using a static 10° height and 10° azimuth angle calculation.
To reduce the number of data records needed while retaining the information of the objects hit, the numbers of facets is reduced with increasing height angles. Since the facet area covered decreases with higher height angles, the resolution of azimuth angles can be reduced using a Sine function
(→ see Figure 2).

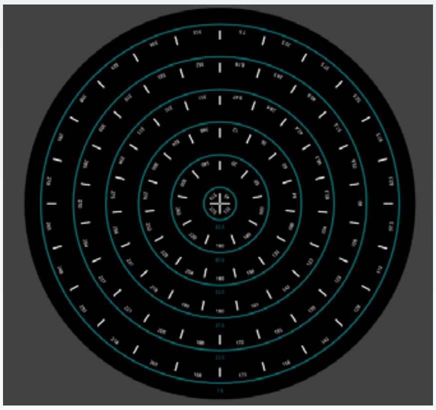

→ **Figure 2**: Upper hemisphere of a IVS analysis. Number of facets for ray tracing reduces with increasing height angle.

This greatly reduces the number of facets for each cell by around 1/3 with almost no loss in accuracy. Furthermore, a dynamic adjustment of the height and azimuth angles was introduced. The user can now set the height angle and azimuth angles resolution in order to save memory.
Comparing simulation results with and without the new IVS algorithm the huge improvements in calculating the actual versus the averaged secondary radiative fluxes becomes apparent. In a small model area, buildings with very different albedos have been digitized.
(→ see Figure 3).

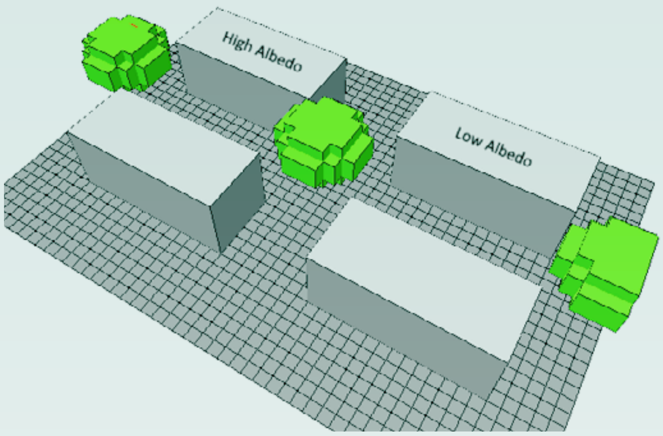

→ **Figure 3:** Model area for comparison simulations. Buildings in the background feature different albedo (left high albedo, right low albedo)

Comparing the distribution of secondary radiative fluxes for the two simulations, it becomes apparent, that in the AVS simulation, no difference in the reflected shortwave radiation caused by the two very different building surfaces can be seen. Furthermore, the pattern of the reflected shortwave radiation stays static over the course of the day and only the absolute values adjust to the generally increasing shortwave radiation between 6 am and 11am
(→ see Figure 4).

Looking at the new IVS outputs, not only the effects of the two different building types with higher reflections in front of the high albedo building is visible, but also the sun angle dependent changes in the radiation patterns become apparent
(→ see Figure 5).

This of course also changes the radiative fluxes in the street canyon, where in the AVS simulation a rather homogenous pattern of reflected shortwave radiation can be found, the model outputs of the IVS simulation clearly shows the effect of the high albedo buildings. **(→ see Figure 6)**

ENVI
_MET

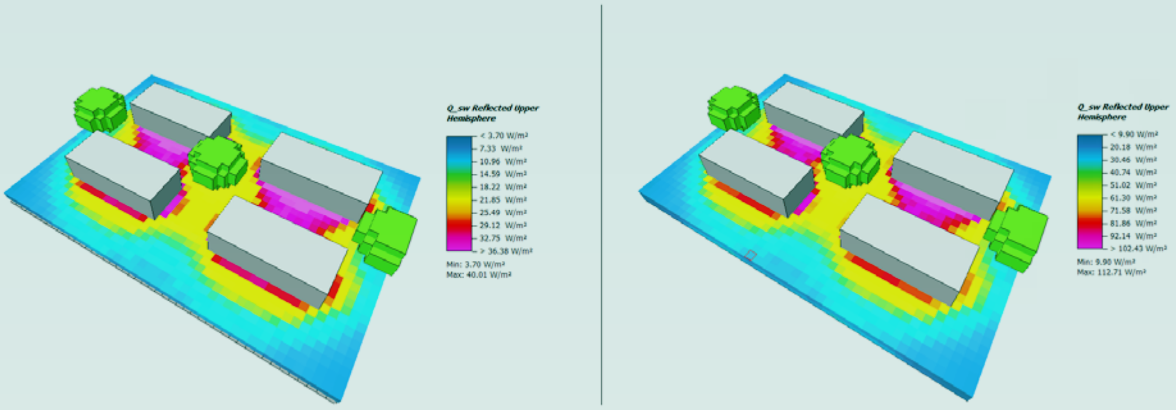

→ **Figure 4**: Pattern of reflected shortwave radiation in the AVS simulation.
Left: Model output at 6 am; Right: Model output at 11 am

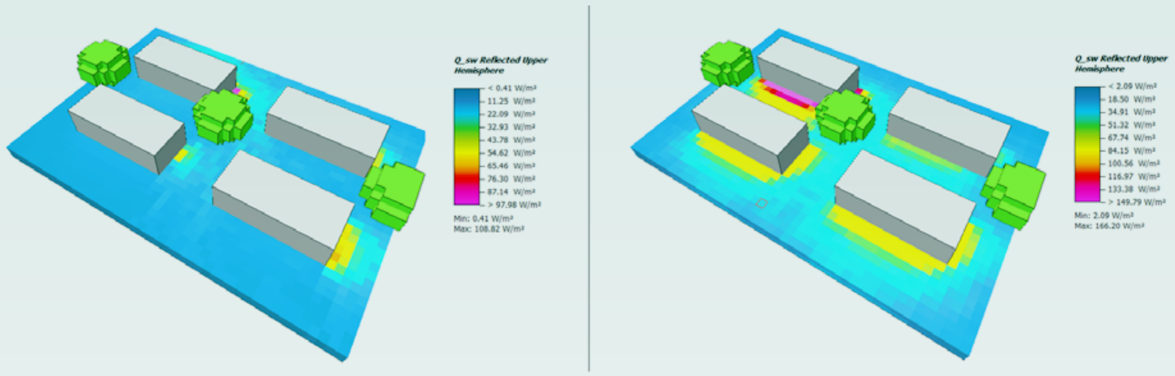

→ **Figure 5**: Pattern of reflected shortwave radiation in the IVS simulation.
Left: Model output at 6 am; Right: Model output at 11 am

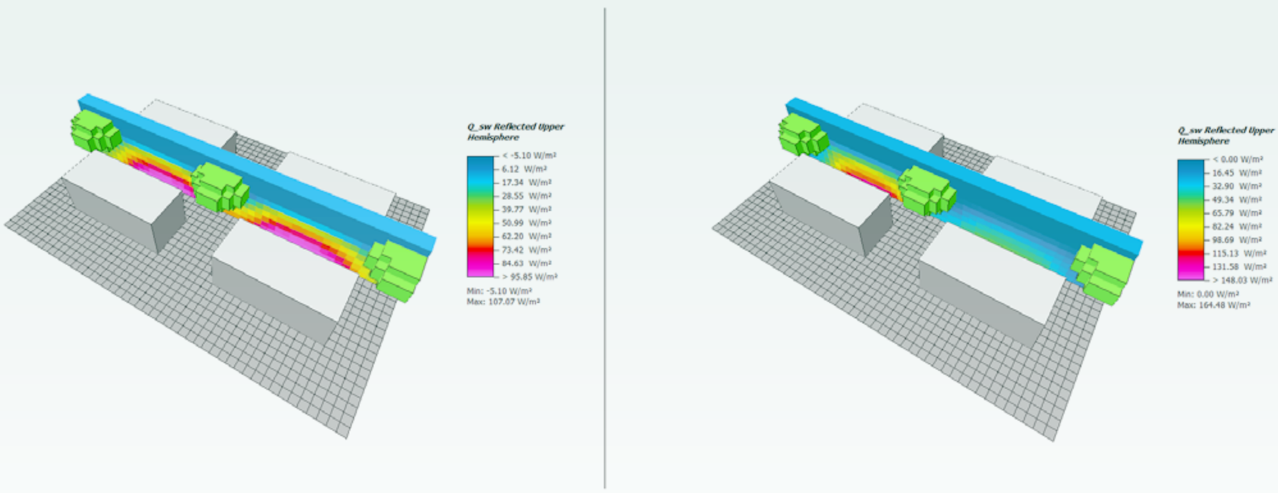

→ **Figure 6**: Reflected shortwave radiation fluxes in street canyon at 13pm simulation time. AVS simulation left; IVS simulation right